Human talar and femoral cartilage have distinct mechanical properties near the articular surface

Corinne R. Henak [a,1], Keir A. Ross [b], Edward D. Bonnevie [c], Lisa A. Fortier [d], Itai Cohen [e], John G. Kennedy [b], Lawrence J. Bonassar [a,c,*]

[a] Meinig School of Biomedical Engineering, Cornell University, Ithaca, NY, United States
[b] Hospital for Special Surgery, New York, NY, United States
[c] Sibley School of Mechanical and Aerospace Engineering, Cornell University, Ithaca, NY, United States
[d] Department of Clinical Sciences, Cornell University, Ithaca, NY, United States
[e] Department of Physics, Cornell University, Ithaca, NY, United States

ABSTRACT

Talar osteochondral lesions (OCL) frequently occur following injury. Surgical interventions such as femoral condyle allogeneic or autogenic osteochondral transplant (AOT) are often used to treat large talar OCL. Although AOT aims to achieve OCL repair by replacing damaged cartilage with mechanically matched cartilage, the spatially inhomogeneous material behavior of the talar dome and femoral donor sites have not been evaluated or compared. The objective of this study was to characterize the depth-dependent shear properties and friction behavior of human talar and donor-site femoral cartilage. To achieve this objective, depth-dependent shear modulus, depth-dependent energy dissipation and coefficient of friction were measured on osteochondral cores from the femur and talus. Differences between anatomical regions were pronounced near the articular surface, where the femur was softer, dissipated more energy and had a lower coefficient of friction than the talus. Conversely, shear modulus near the osteochondral interface was nearly indistinguishable between anatomical regions. Differences in energy dissipation, shear moduli and friction coefficients have implications for graft survival and host cartilage wear. When the biomechanical variation is combined with known biological variation, these data suggest the use of caution in transplanting cartilage from the femur to the talus. Where alternatives exist in the form of talar allograft, donor-recipient mechanical mismatch can be greatly reduced.

© 2016 Published by Elsevier Ltd.

1. Introduction

Talar osteochondral lesions (OCL) have been reported with increasing frequency, due to higher resolution imaging and increasing sporting activity in an aging population. Most talar OCL result from a traumatic event, typically an ankle sprain. An estimated 50% of significant ankle sprains result in some form of cartilaginous injury (Ferkel and Chams, 2007; Saxena and Eakin, 2007; Takao et al., 2005). Of these OCL, 50% require some form of surgical intervention (Zengerink et al., 2010).

The long-term aim of OCL treatment is to restore the mechanical function of native talar cartilage, and to thereby prevent or delay progression of joint degeneration (Zengerink et al., 2010). To achieve this aim, two broad treatment options are available; either to repair the cartilage or replace it. While reparative strategies, including microfracture and microdrilling, have shown good short to medium term clinical outcomes, longer term outcomes in larger lesions are less promising (Savage-Elliott et al., 2014).

Larger talar OCL are typically treated by replacing defective cartilage and bone with an allogeneic or autologous osteochondral transplant (AOT), typically from the ipsilateral femoral condyle. Clinical outcomes following AOT have been excellent with functional scores of 90% or greater being reported in short and medium term outcome studies (Hangody et al., 2008; Valderrabano et al., 2009). Despite these excellent functional outcomes, concern remains regarding long term implications of mismatches in mechanical behavior between recipient and donor cartilage. Radiographic outcomes in several studies suggest that biologic integration between host and graft may not be optimal. For example, cyst formation in the subchondral bone has been shown

---

in 67% of patients at a minimum of 43 months follow-up (Valderrabano et al., 2009), with biologic intervention via bone marrow aspirate insufficient to completely prevent their development (Kennedy and Murawski, 2011).

Further, previous cadaveric studies evaluating mechanical implications of graft placement have demonstrated that an elevated graft leads to increased contact pressure on the graft, while a graft of matched articular surface topology results in increased contact pressures in surrounding recipient cartilage (Fansa et al., 2011; Latt et al., 2011). This mismatch in cartilage contact mechanics may result in part from a fundamental mismatch in cartilage mechanical behavior between donor and graft cartilage. Recently, greater attention has being given to allogenic osteochondral grafts in the treatment of OCL (Görtz et al., 2010; Janis et al., 2010). This is in part due to the concern of donor site morbidity from autograft harvesting from the knee and in part because of increasing availability and greater safety associated with allografts than previously achievable (Mroz et al., 2008; Savage-Elliott et al., 2014). The possibility exists that topographical variability, cartilage thickness, and mechanical properties between ankle and knee cartilage could be better matched if areas of the talus could be compared to areas of the distal femur. This would allow the surgeon an *á la carte* choice of femoral graft depending on the location of the talar OCL.

Cartilage exhibits a wide variety of depth- and location-dependent complex material behaviors. Shear and equilibrium cartilage moduli are substantially larger near the osteochondral interface than near the articular surface (Buckley et al., 2013, 2008; Chen et al., 2001; Wong and Sah, 2010; Wong et al., 2008a, 2008b), resulting in larger shear strains at the articular surface than in the bulk of the tissue (Wong and Sah, 2010; Wong et al., 2010, 2008a, 2008b). Further, most energy dissipation within cartilage occurs near the articular surface (Buckley et al., 2013, 2008). Spatial heterogeneity in depth-dependent cartilage mechanical properties have been reported in immature bovine knees (Silverberg et al., 2013), but such variations have not been investigated in human knees and ankles. Talar AOT grafts are commonly obtained from the patient's ipsilateral femoral condyle, although neither the biological nor the bulk mechanical properties match those of talar cartilage (Aurich et al., 2005; Fetter et al., 2006; Quinn et al., 2013; Schumacher et al., 2002; Treppo et al., 2000). To date, neither the depth-dependent mechanical behavior of native ankle cartilage nor that of potential graft tissue from unloaded regions of the knee has been well characterized. Therefore, the objective of this study was to characterize the depth-dependent shear properties and friction properties of human talar and donor-site femoral cartilage, and to establish the extent of variation in mechanical properties between these locations.

2. Materials and methods

2.1. Specimens

Nine tali and nine femurs were obtained from 14 cadaveric lower limbs (Table 1). Cadaveric tissue was obtained from an anatomic donation organization. During dissection, cartilage was screened for gross abnormality; macroscopically normal cartilage was used. Osteochondral cores were removed from nine talar anatomical regions (Elias et al., 2007) as well as from the superomedial and superolateral trochlear groove, common femoral donor-sites, using an 8 mm coring tool (Fig. 1A and B). Femoral locations were selected because of their common use as donor tissue in AOT procedures, in contrast to previous studies that have characterized mechanical behavior of weight-bearing regions (Wong and Sah, 2010; Wong et al., 2010, 2008a, 2008b). Samples were frozen at −80 °C between dissection and testing. Cylindrical cores were split into three samples: a 4 mm diameter osteochondral sample for tribology, a partial cylinder for shear, and the remainder for histology in a subset of samples (Fig. 1C).

Table 1

Specimen characteristics. An 'X' marks joints that were used in this study. Each ankle provided nine samples and each knee provided two samples.

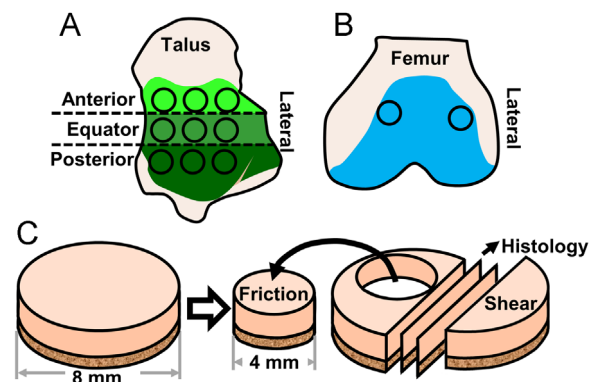| Specimen	Gender	Age (years)	BMI (kg m^{-2})	Ankle		Knee	
				L	R	L	R
1	M	57	17		X		
2	F	47	23	X	X		
3	F	52	23	X			
4	F	47	24			X	X
5	M	69	19			X	
6	M	63	26				X
7	M	71	35			X	
8	M	75	35				X
9	M	60	25	X			
10	F	59	27		X		X
11	F	60	21	X		X	
12	M	48	18		X		
13	M	55	35	X			
14	M	49	30				X

Fig. 1. (A) Osteochondral cores were removed from three anatomical regions on the talus, with three cores from each region. (B) Osteochondral cores were removed from two common donor-site locations on the femur. (C) Each sample was further divided into a 4 mm diameter sample for friction testing and a partial cylinder for shear testing. The remainder of a subset of samples was fixed and sectioned for histology.

2.2. Shear testing

Shear behavior was characterized using confocal elastography on a custom test device (Buckley et al., 2013, 2008) (Fig. 2A). Bone was trimmed to create a subchondral surface plane parallel to the articular surface, as confirmed visually under confocal microscopy (Buckley et al., 2008). Samples were stained in 28 μM 5-DTAF (Invitrogen, Waltham, MA) for 1–2 h. Following staining, samples were rinsed in PBS for 10 min to remove unbound dye. Samples were mounted on a custom backplate using cyanoacrylate. The moving front plate was sandblasted glass to provide a no-slip condition between the front plate and the cartilage following axial compression (Buckley et al., 2013). Cartilage thickness was measured under confocal microscopy; measurements were taken three times across the sample width and averaged. Samples were compressed axially and allowed to creep until reaching equilibrium, resulting in a final axial compression of 7.9 ± 0.7% (range, 6.8–9.7%). One to five lines were photobleached perpendicular to the articular surface (Fig. 2B). Cyclic shear loading was applied, using 1% shear strain at 1 Hz. While shear behavior varies with loading frequency (Buckley et al., 2013), 1 Hz was selected for its relevance to walking (Silverberg et al., 2013). Displacement of the photobleached lines was imaged during loading at 20 frames per second. After loading, the axial cross-sectional area was imaged for stress calculations.

Depth-dependent shear modulus, phase angle and energy dissipation were calculated using established methods (Buckley et al., 2013). Depth-dependent displacement of photobleached lines was tracked using custom code in MatLab (The MathWorks, Inc., Natick, MA), then used to calculate depth-dependent shear strain, shear modulus, phase angle and energy dissipation, by fitting displacement with a cosine function as described by Buckley et al. (2013).

Well-defined points on depth-dependent curves were obtained to compare between regions. Minimum and plateau shear moduli were evaluated (Fig. 2C). The minimum value was the global minimum; consistent with previous studies using different cartilage sources this typically occurred near the articular surface (Buckley et al., 2013, 2010; Silverberg et al., 2013). Plateau shear modulus was the average of
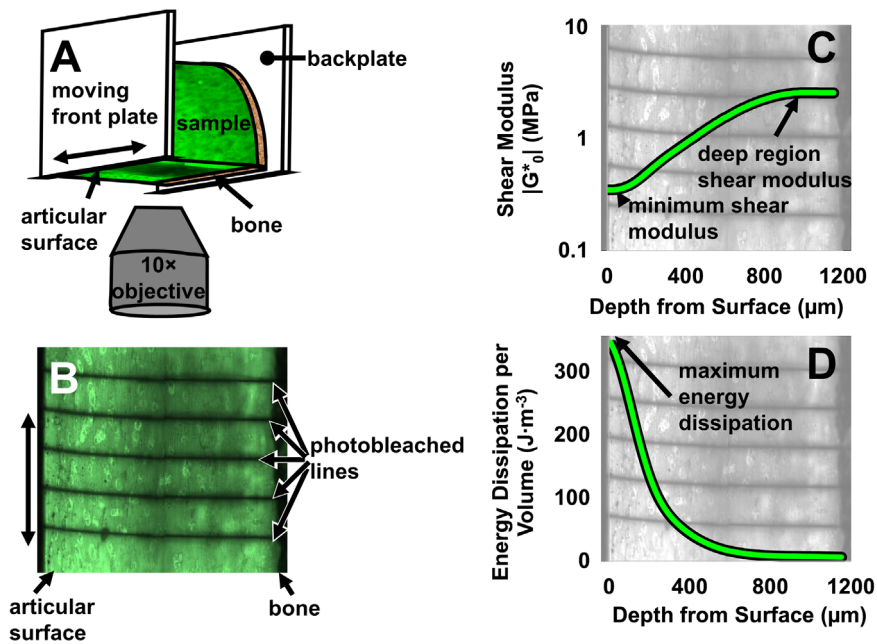
Fig. 2. Overview of shear methods. (A) Partial cylinder samples were glued to a stationary backplate, compressed axially, and sheared by a moving front plate. Images were captured during deformation using a $10 \times$ objective. (B) Confocal images demonstrated the location of photobleached lines as a function of time. The vertical line displacement was used to calculate depth-dependent mechanics. (C) Shear modulus, $|G^{*}_{0}|$, as a function of cartilage depth, overlaid with a single frame from the corresponding sample. Arrows demonstrate the minimum shear modulus near the articular surface and the deep region shear modulus, a region of nearly constant shear modulus near the bone. (D) Energy dissipation as a function of cartilage depth demonstrates that the maximum energy dissipation occurs near the articular surface.

the values where the slope of the shear modulus dropped off. Cartilage thickness, measured prior to compression, was compared. Maximum energy dissipation, the peak depth-dependent value, (Fig. 2D) and total energy dissipation through the cartilage depth were calculated.

2.3. Tribology

Intrinsic boundary mode coefficient of friction of each sample was determined using a custom tribometer and established methods (Gleghorn and Bonassar, 2008). Boundary mode was selected for analysis because of its consistency across studies with different counterfaces (Abubacker et al., 2015; Gleghorn and Bonassar, 2008; Schmidt et al., 2007). Cylindrical cartilage samples were attached to pivoting mounts and compressed against a polished glass surface in a PBS bath. Samples were compressed 30% axially and allowed to relax for 60 min. Following relaxation, samples were translated laterally at 0.3 mm s^{-1} while normal and shear forces were measured from a biaxial load cell. Friction coefficients were measured from the ratio of shear to normal force. Reported values are averages from the second and third of three cycles.

2.4. Histology

To provide confidence that differences between samples were due to anatomical variation and not due to degenerative changes, a subset of samples were histologically evaluated. Sections were fixed in 10% formalin for 48 h, then moved to 10% EDTA to decalcify the bone. Samples were checked radiographically every two days after one week in EDTA and moved to 70% EtOH when fully decalcified. Samples were sectioned to 4 μm for staining (Fig. 1C). Samples were stained with safranin-O/fast green to evaluate glycosaminoglycan (GAG) distribution, hematoxylin and eosin (H&E) to evaluate cell distribution and nuclear morphology, and picrosirius red to evaluate collagen distribution. Safranin-O/fast green and H&E slides were viewed under white light and picrosirius red slides were viewed under polarized light. Samples were scored using established scales for cell, matrix, and collagen features (Changoor et al., 2011; McIlwraith et al., 2010; Pritzker et al., 2006). The score for collagen features was based solely on polarized light images and was inverted from the established scale such that healthy cartilage was scored as zero. Each feature was scored independently and averaged for the overall histological score. All scores were completed by a single investigator (CRH).

2.5. Statistics

To assess the appropriateness of femoral and talar donor AOT graft for talar repair, mechanical variables, thickness, and histological scores were compared using a multilevel mixed-effects linear regression model that accounted for

repeated donors (UCLA: Statistical Consulting Group n.d.). Comparisons were made between all regions, as well as between the talus and the femur. Model assumptions were checked, and a log transform of the variable was used if assumptions were not met. Linear regression was used to evaluate correlation between variables. Statistical analyses were completed in Stata (StataCorp LP, College Station, TX). Repeated measures were corrected via Finner's procedure (Finner, 1993); corrected P values are reported.

3. Results

Both shear modulus and energy dissipation demonstrated distinct depth-dependent variation, with deep region shear moduli 48-fold larger than shear moduli near the articular surface on average (Fig. 3A). Variations in depth-dependent shear moduli between anatomical regions primarily occurred within 300 μm of the articular surface. The region nearest the articular surface also exhibited the largest energy dissipation (Fig. 3B).

The femur was softer than the talus near the articular surface, but all regions were nearly identical near the osteochondral interface (Fig. 4A and B). The minimum shear modulus, which occurred near the articular surface, was 4.4-fold lower in the femur than in the talus ($P=0.021$). On average, minimum femoral shear moduli were 3.6-, 5.4-, and 4.1-fold lower than the anterior, equator and posterior talar regions, respectively (Fig. 4A) ($0.1 < P < 0.15$). Minimum shear moduli were nearly identical within the talus ($P > 0.7$). Deep region shear moduli were consistent across all regions (Fig. 4B) ($P \geq 0.2$).

Energy dissipation was lower in the anterior talus than in all other regions, and trended towards being lower in the commonly injured, equator talus (Elias et al., 2007) than in the femur (Fig. 4C). Specifically, maximum energy dissipation in the anterior talus was 1.7–2.5-fold lower than all other regions ($P \leq 0.001$). Maximum energy dissipation in the femur showed a trend towards being higher than in the equator talus ($P=0.083$), but was not different than in the posterior talus ($P=0.359$). Similarly, energy dissipation was indistinguishable between the equator and posterior talus ($P=0.359$). Overall, femoral maximum energy
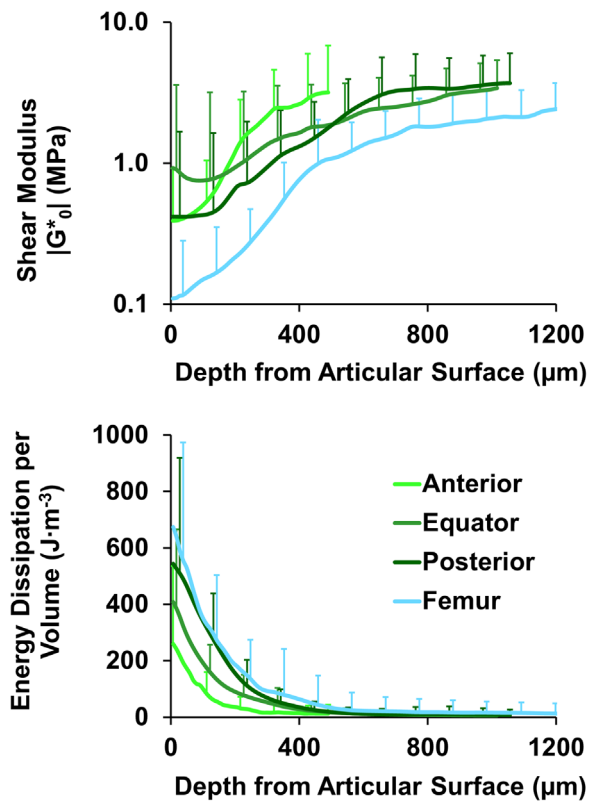
Fig. 3. Results as a function of cartilage depth ($n=18$ in femur, $n=27$ in each talus region). Articular surface is at zero depth. (A) Depth-dependent shear modulus. Femoral cartilage was 4.4 times softer near the articular surface than talar cartilage. In the deeper portion of the tissue, all regions converged to a similar magnitude plateau. (B) Depth-dependent energy dissipation per volume. Error bars=standard deviation.
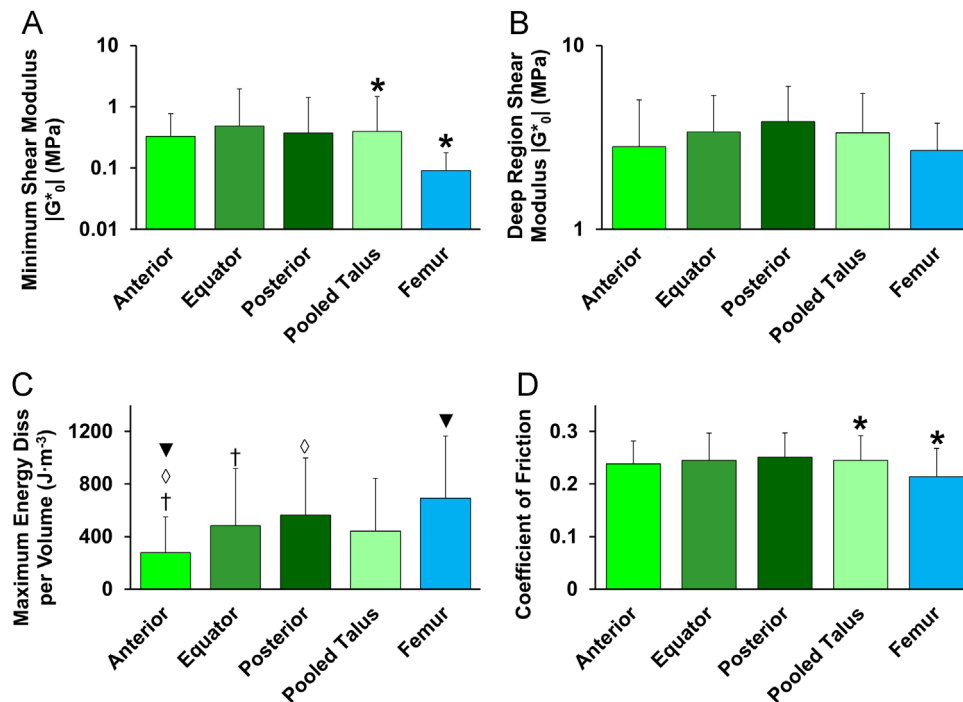
dissipation showed a trend towards being higher than talar maximum energy dissipation ($P=0.087$). Trends in total energy dissipation mirrored those of maximum energy dissipation (results not shown).

The femur had a lower boundary mode coefficient of friction than the talus ($P=0.036$). Friction coefficients were not significantly different between the three talar regions and the femur (Fig. 4D) ($P \geq 0.16$). The coefficient of friction was nearly identical within talar regions ($P > 0.8$).

While select variables demonstrated significant correlations, neither thickness nor deep region modulus fully explained articular surface mechanics (Fig. 5). Relationships were demonstrated through linear correlations, which had uniformly low R^2 values. Thickness was poorly correlated with minimum shear modulus and coefficient of friction ($P > 0.2$, $R^2=0.02$), but was significantly correlated with maximum energy dissipation per volume (Fig. 5A–C) ($P < 0.001$, $R^2=0.16$). Deep region shear modulus was significantly correlated with minimum shear modulus (Fig. 5D) ($P=0.02$, $R^2=0.07$), but poorly correlated with coefficient of friction and maximum energy dissipation per volume (Fig. 5E and F) ($P > 0.45$, $R^2 \leq -0.01$). Low R^2 values indicate that thickness and deep region shear modulus account for less than 20% of the variation in energy dissipation, minimum shear modulus and friction coefficient.

Cartilage thickness varied significantly between all regions. Femoral cartilage was thicker than talar cartilage ($P < 0.001$). Cartilage was thinnest anteriorly, increased posteriorly and was thicker in the femur than in all talar regions ($P=0.003$ for anterior versus equator; $P < 0.001$ for all other comparisons). Anterior talar cartilage was 1.03 ± 0.28 mm thick (range, 0.55–1.66 mm), equator talar cartilage was 1.48 ± 0.25 mm thick (range, 1.10–2.22 mm), posterior talar cartilage was 1.62 ± 0.33 mm thick (range, 1.17–

Fig. 4. Regional differences in cartilage mechanics ($n=18$ in femur, $n=27$ in each talus group, $n=81$ in pooled talus). (A) Minimum shear modulus, occurring near the articular surface, was softer in the femur than in the pooled talus. (B) Deep region shear moduli were indistinguishable between regions. (C) Maximum energy dissipation was smaller in the anterior talus than in all other regions. (D) Coefficient of friction, measured at the articular surface, was lower in the femur than in the pooled talus. Matched symbols indicate $P \leq 0.05$. Error bars=standard deviation.
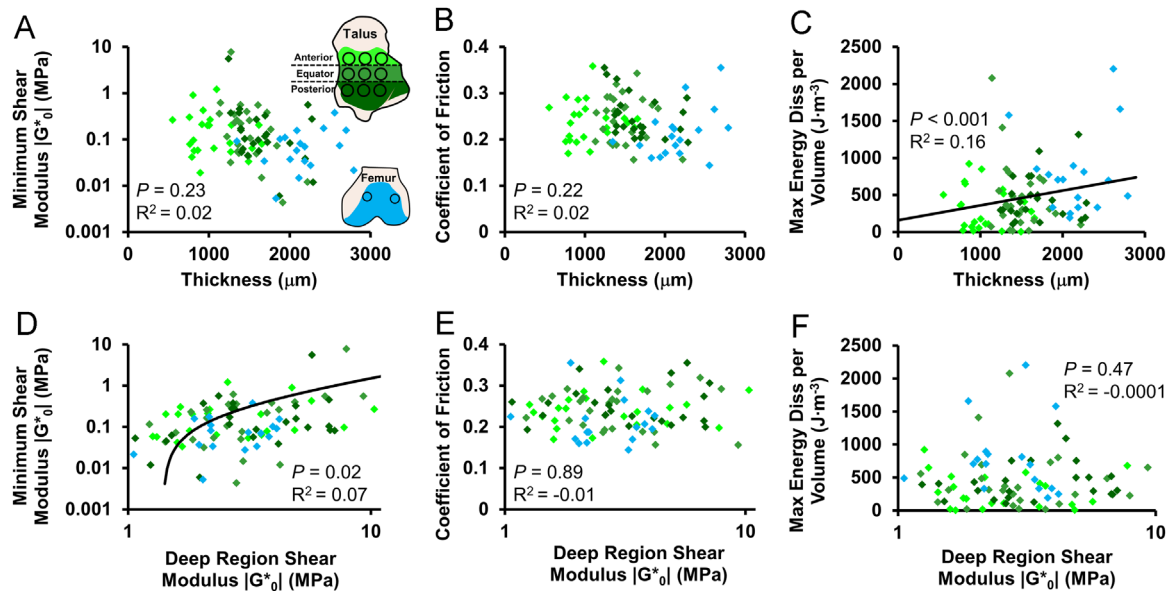
Fig. 5. Correlations between values that can be acquired with clinical imaging and mechanical variables at the articular surface ($n=99$). (A) Minimum shear modulus versus thickness. Colors indicate anatomical region as shown in the inset talus and femur. (B) Coefficient of friction versus thickness. (C) Maximum energy dissipation per volume was positively correlated with thickness, but thickness would still be insufficient to accurately predict energy dissipation. (D) Minimum shear modulus was positively correlated with deep region shear modulus, although deep region shear modulus would serve as a poor predictor for the minimum shear modulus. (E) Coefficient of friction versus deep region shear modulus. (F) Maximum energy dissipation per volume versus deep region shear modulus. Solid lines indicate linear correlation.
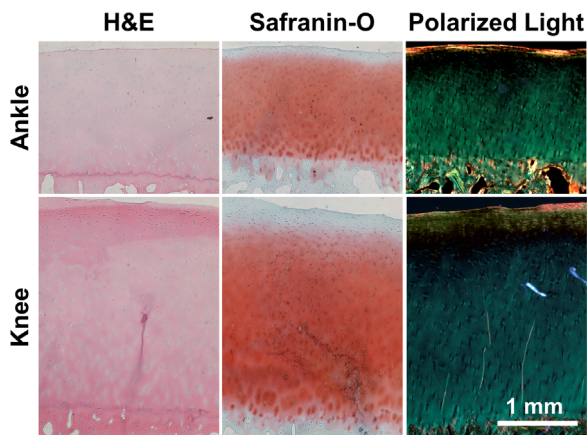

Fig. 6. Representative histological sections of ankle and knee cartilage.

2.29 mm) and femoral cartilage was 2.16 ± 0.37 mm thick (range, 1.35–2.79 mm).

Histological scores, used to check for cartilage degeneration, were consistent across regions and did not correlate with any other variables (Fig. 6). Histological scores were 1.48 ± 0.23, 1.40 ± 0.17, 1.34 ± 0.19, and 1.52 ± 0.23 for the anterior, equator, posterior and femur cartilage, respectively (ranges, 1.19–2.13, 1.19–1.69, 1.13–1.81 and 1.31–1.94, respectively; healthy cartilage was scored zero). Differences between regions were not significant ($P \geq 0.17$). Histological score was not significantly correlated with any other variable ($P \geq 0.14$).

4. Discussion

Both autogeneous and allogeneic AOT are common methods of treating large talar lesions. While short term clinical outcomes have been promising, concern has recently arisen regarding the presence of post-operative subchondral cysts seen radiographically at medium term follow up, in up to ⅔ of patients undergoing talar AOT (Adams et al., 2011; Görtz et al., 2010; Haene

et al., 2012; Valderrabano et al., 2009). Cystic changes in the subchondral bone are a concern as a harbinger of progressive subchondral bone and graft collapse. While cystic changes may reflect mechanical variance between donor femoral and recipient talar cartilage, the specific mechanical differences between talar and donor-site femoral cartilage have not been elucidated or previously investigated. The current study identified differences between femoral and talar cartilage material properties, with most differences concentrated within 300 μm of the articular surface.

Differences in mechanical behavior near the articular surface suggest that clinical autograft failure (Kim et al., 2012) may result from stress shielding or stress concentrations, and mismatches in energy absorption and wear. Because cartilage layers are in contact within the joint, the relative behavior of donor and recipient cartilage would be expected to result in failure in different anatomical regions of the ankle joint. Shear deformation is important for chondrocyte viability and cartilage failure (Atkinson et al., 1998a, 1998b; Hashimoto et al., 2009; Smith et al., 2004). Further, cartilage contact results in both compressive and shear deformation within the tissue, making shear moduli relevant for normal joint loading. Thus, differences in minimum shear modulus may be important for AOT graft failure. Differences in shear modulus between the femur and talus also account for lower contact pressures seen on graft cartilage in previous cadaveric studies (Fansa et al., 2011; Latt et al., 2011). Energy dissipation appears to be a mechanism that cartilage uses to protect itself from damage (Bartell et al., 2015; Buckley et al., 2013). Energy dissipation near the articular surface was greater in femoral than in talar cartilage, suggesting that femoral cartilage would be relatively protected when transplanted to the talus. For a surface with a higher coefficient of friction, that surface and the surface it slides against may be more susceptible to wear. Further, elevated friction coefficients lead to increased chondrocyte apoptosis (Waller et al., 2013). Thus, the lower coefficient of friction in the femur than in the talus suggests damage on cartilage mated to native talar cartilage following autogeneous AOT. While biological differences were not evaluated in this study, previously established biological differences between ankle and knee cartilage, such as cell morphology, cell density, and cartilage metabolism (Aurich et al., 2005; Quinn

et al., 2013; Schumacher et al., 2002) further underscore concerns about transferring cartilage grafts from the femur to the talus.

The mechanical mismatch between femoral and talar cartilage occurred exclusively near the articular surface. This suggests the importance of matching articular surface properties and of maintaining articular surface integrity in AOT surgery. While short term clinical outcomes have been encouraging following autogeneous AOT, the authors are unaware of studies with follow-up greater than ten years (Adams et al., 2011; Berlet et al., 2011; Görtz et al., 2010; Gross et al., 2001; Haene et al., 2012; Hahn et al., 2010; Hangody et al., 2008; Meehan et al., 2005; Raikin, 2009; Valderrabano et al., 2009). Concern over subchondral cyst formation following AOT has been stated, although whether this phenomenon causes long term failure is unknown. The mismatch in mechanical properties of femoral and talar cartilage suggest that advantages of autogenous graft should be carefully examined, particularly in light of increasing availability and decreased immune concerns of allograft (Mroz et al., 2008). The current study demonstrated that variations in mechanical and topographical characteristics in femoral condyle cartilage according to harvest site can be chosen to more accurately represent talar areas affected by OCL.

In addition to inter-region variation, substantial intra-region variation that cannot be predicted by clinical imaging was revealed. Currently, magnetic resonance imaging can quantify cartilage thickness and provide information regarding cartilage quality that is correlated to material behavior (El-Khoury et al., 2004; Juras et al., 2009; Tang et al., 2011). While thickness was significantly correlated with energy dissipation and deep region shear modulus was significantly correlated with minimum shear modulus, the spread in mechanical variables near the articular surface prohibits either thickness or deep region shear modulus from being highly predictive. Further, the resolution required to characterize depth-dependent variations in material behavior within talar cartilage is not yet available (Burge et al., 2012; Juras et al., 2009; Tang et al., 2011). Differences between regions in articular surface mechanics coupled with current clinical imaging resolution and known correlations between composition and depth-dependent shear behavior (Silverberg et al., 2014) suggests that ongoing research focus on increasing the resolution of cartilage structural information obtained from magnetic resonance imaging.

This study reiterates the uniqueness of the articular surface and adjacent cartilage, where differences between joints may have implications in differences in osteoarthritis prevalence. Shear moduli of deep regions of cartilage were nearly identical between anatomical regions, while shear moduli near the articular surface varied between anatomical regions. This is consistent with previous research, where regional variations in shear properties in the neonatal bovine stifle were focused near the articular surface (Silverberg et al., 2013). The magnitudes of shear moduli, energy dissipation, and friction coefficient are consistent with previous studies (Buckley et al., 2013; Gleghorn and Bonassar, 2008; Silverberg et al., 2013). Together, these results demonstrate that the uniqueness of the articular surface, both in comparison to the bulk tissue and in comparison between anatomical regions, is preserved across joints, species, maturity and joint-level loading patterns. Within the human ankle and knee, previous research has found lower equilibrium and dynamic moduli in knee cartilage than in ankle cartilage for the most superficial 1 mm of tissue (Treppo et al., 2000). The localization of differences in shear moduli near the articular surface suggests that previously described differences primarily resulted from superficial zone discrepancies. Maximum energy dissipation, which also occurs near the articular surface, was larger in the femur than in the talus. The coefficient of friction, measured at the articular surface, was smaller in the femur than in the talus. While the mechanism for this difference was not addressed in the present study, previous research suggests that this difference may be driven by differences in lubricin and surface roughness between anatomical locations (DuRaine et al., 2009; Gleghorn et al., 2009; Peng et al., 2015). In addition to the concentration of mechanical differences near the articular surface, the superficial zone is also the location of differences in cell density between the ankle and knee (Quinn et al., 2013). As the initiation of osteoarthritic damage occurs at the articular surface (Hollander et al., 1995), the current study combined with previous data suggest that mechanical and biological differences near the surface may be important factors that modulate damage in these joints.

This study has limitations. During autograft AOT, matched femoral cartilage is used but femoral and talar cartilage was not matched for all donors in this study. Previous research demonstrating differences in cartilage thickness in matched pairs (Shepherd and Seedhom, 1999) suggests that mechanical differences would remain if matched pairs were analyzed. Due to processing errors, histology was not completed on all specimens. However, histological scores were consistent for processed samples and all samples were sourced using the same methods, suggesting that degenerative changes would be consistent across samples. Friction properties were measured in PBS, rather than in synovial fluid. Previous research shows that synovial fluid decreases the friction coefficient (Gleghorn and Bonassar, 2008); and that the interaction between lubricin and hyaluronic acid is synergistic (Bonnevie et al., 2015). Thus, specifically how synovial fluid would affect the differences in friction coefficients measured in the present study is difficult to predict, given the potential variation in bound lubricin and available binding sites between the different anatomical locations. This study focused on shear and friction properties, but cartilage also experiences compressive deformation in vivo. Depth-dependent variation in compressive modulus is consistent with depth-dependent variation in shear modulus (Schinagl et al., 1997), and there is generally more information already available about cartilage compressive behavior. Further, the compressive modulus can be calculated from the shear modulus and Poisson's ratio in the linear regime. The testing methods used in this study do not mimic in vivo conditions, but instead provide information on the intrinsic material behavior. Finally, the importance of specific mechanical properties to the long-term success of grafts is unclear; differences in shear modulus, energy dissipation, and friction coefficient at the time of osteochondral transplant surgery will not necessarily predict graft or recipient cartilage failure.

In conclusion, clear biomechanical differences exist between femoral cartilage and talar cartilage, especially near the articular surface. Differences in energy dissipation, shear moduli and friction coefficients have implications for graft survival and host cartilage wear, and may be mechanisms through which AOT grafts fail. When biomechanical variation is combined with biological variation, the authors urge caution in transplanting cartilage from the femur to the talus. Where alternatives exist in the form of talar allograft, donor-recipient mechanical mismatch can be greatly reduced. Long term clinical studies will be required to substantiate the clinical outcomes of these findings.

Conflict of interest statement

The authors have no conflicts of interest that could bias this research.

Acknowledgments

References

Abubacker, S., Dorosz, S.G., Ponjevic, D., Jay, G.D., Matyas, J.R., Schmidt, T.A., 2015. Full-length recombinant human proteoglycan 4 interacts with hyaluronan to provide cartilage boundary lubrication. Ann. Biomed. Eng. http://dxdoi.org/10.1007/s10439-015-1390-8

Adams, S.B., Viens, N.A., Easley, M.E., Stinnett, S.S., Nunley, J.A., 2011. Midterm results of osteochondral lesions of the talar shoulder treated with fresh osteochondral allograft transplantation. J. Bone Jt. Surg. Am. 93, 648–654. http://dx.doi.org/10.2106/JBJS.J.00141.

Atkinson, T., Haut, R., Altiero, N., 1998a. Impact-induced fissuring of articular cartilage: an investigation of failure criteria. J. Biomech. Eng. 120, 181–187.

Atkinson, T., Haut, R., Altiero, N., 1998b. An investigation of biphasic failure criteria for impact-induced fissuring of articular cartilage. J. Biomech. Eng. 120, 536–537.

Aurich, M., Squires, G.R., Reiner, A., Mollenhauer, J.A., Kuettner, K.E., Poole, A.R., Cole, A.A., 2005. Differential matrix degradation and turnover in early cartilage lesions of human knee and ankle joints. Arthritis Rheum. 52, 112–119. http://dx.doi.org/10.1002/art.20740.

Bartell, L.R., Fortier, L.A., Bonassar, L.J., Cohen, I., 2015. Measuring microscale strain fields in articular cartilage during rapid impact reveals thresholds for chondrocyte death and a protective role for the superficial layer. J. Biomech. 48, 3440–3446. http://dx.doi.org/10.1016/j.jbiomech.2015.05.035.

Berlet, G.C., Hyer, C.F., Philbin, T.M., Hartman, J.F., Wright, M.L., 2011. Does fresh osteochondral allograft transplantation of talar osteochondral defects improve function? Clin. Orthop. Relat. Res. 469, 2356–2366. http://dx.doi.org/10.1007/s11999-011-1813-2.

Bonnevie, E.D., Galesso, D., Secchieri, C., Cohen, I., Bonassar, L.J., 2015. Elastoviscous transitions of articular cartilage reveal a mechanism of synergy between lubricin and hyaluronic acid. PLoS One 10, e0143415. http://dx.doi.org/10.1371/journal.pone.0143415.

Buckley, M.R., Bergou, A.J., Fouchard, J., Bonassar, L.J., Cohen, I., 2010. High-resolution spatial mapping of shear properties in cartilage. J. Biomech. 43, 796–800. http://dx.doi.org/10.1016/j.jbiomech.2009.10.012.

Buckley, M.R., Bonassar, L.J., Cohen, I., 2013. Localization of viscous behavior and shear energy dissipation in articular cartilage under dynamic shear loading. J. Biomech. Eng. 135, 31002–1 – 31002–9. http://dx.doi.org/10.1115/1.4007454.

Buckley, M.R., Gleghorn, J.P., Bonassar, L.J., Cohen, I., 2008. Mapping the depth dependence of shear properties in articular cartilage. J. Biomech. 41, 2430–2437. http://dx.doi.org/10.1016/j.jbiomech.2008.05.021.

Burge, A.J., Gold, S.L., Potter, H.G., 2012. Imaging of sports-related midfoot and forefoot injuries. Sport. Heal. A Multidiscip. Approach 4, 518–534. http://dx.doi.org/10.1177/1941738112459489.

Changoor, A., Tran-Khanh, N., Méthot, S., Garon, M., Hurtig, M.B., Shive, M.S., Buschmann, M.D., 2011. A polarized light microscopy method for accurate and reliable grading of collagen organization in cartilage repair. Osteoarthr. Cartil. 19, 126–135. http://dx.doi.org/10.1016/j.joca.2010.10.010.

Chen, A.C., Bae, W.C., Schinagl, R.M., Sah, R.L., 2001. Depth- and strain-dependent mechanical and electromechanical properties of full-thickness bovine articular cartilage in confined compression. J. Biomech. 34, 1–12. http://dx.doi.org/10.1016/S0021-9290(00)00170-6.

DuRaine, G., Neu, C.P., Chan, S.M.T., Komvopoulos, K., June, R.K., Reddi, A.H., 2009. Regulation of the friction coefficient of articular cartilage by TGF-??1 and IL-1??. J. Orthop. Res. 27, 249–256. http://dx.doi.org/10.1002/jor.20713.

Elias, I., Zoga, A.C., Morrison, W.B., Besser, M.P., Schweitzer, M.E., Raikin, S.M., 2007. Osteochondral lesions of the talus: localization and morphologic data from 424 patients using a novel anatomical grid scheme. Foot Ankle Int. 28, 154–161. http://dx.doi.org/10.3113/FAI.2007.0154.

El-Khoury, G.Y., Alliman, K.J., Lundberg, H.J., Rudert, M.J., Brown, T.D., Saltzman, C.L., 2004. Cartilage thickness in cadaveric ankles: measurement with double-contrast multi-detector row CT arthrography versus MR imaging. Radiology 233, 768–773. http://dx.doi.org/10.1148/radiol.2333031921.

Fansa, A.M., Murawski, C.D., Imhauser, C.W., Nguyen, J.T., Kennedy, J.G., 2011. Autologous osteochondral transplantation of the talus partially restores contact mechanics of the ankle joint. Am. J. Sport. Med. 39, 2457–2465. http://dx.doi.org/10.1177/0363546511419811.

Ferkel, R.D., Chams, R.N., 2007. Chronic lateral instability: arthroscopic findings and long-term results. Foot Ankle Int. 28, 24–31. http://dx.doi.org/10.3113/FAI.2007.0005.

Fetter, N.L., Leddy, H.A., Guilak, F., Nunley, J.A., 2006. Composition and transport properties of human ankle and knee cartilage. J. Orthop. Res. 24, 211–219. http://dx.doi.org/10.1002/jor.20029.

Finner, H., 1993. On a monotonicity problem in step-down multiple test procedures. J. Am. Stat. Assoc. 88, 920–923.

Gleghorn, J.P., Bonassar, L.J., 2008. Lubrication mode analysis of articular cartilage using Stribeck surfaces. J. Biomech. 41, 1910–1918. http://dx.doi.org/10.1016/j.jbiomech.2008.03.043.

Gleghorn, J.P., Jones, A.R.C., Flannery, C.R., Bonassar, L.J., 2009. Boundary mode lubrication of articular cartilage by recombinant human lubricin. J. Orthop. Res. 27, 771–777. http://dx.doi.org/10.1002/jor.20798.

Görtz, S., De Young, A.J., Bugbee, W.D., 2010. Fresh osteochondral allografting for osteochondral lesions of the talus. Foot ankle Int. 31, 283–290. http://dx.doi.org/10.3113/FAI.2010.0283.

Gross, A.E., Agnidis, Z., Hutchison, C.R., 2001. Osteochondral defects of the talus treated with fresh osteochondral allograft transplantation. Foot ankle Int. 22, 385–391.

Haene, R., Qamirani, E., Story, R.A., Pinsker, E., Daniels, T.R., 2012. Intermediate outcomes of fresh talar osteochondral allografts for treatment of large osteochondral lesions of the talus. J. Bone Jt. Surg. Am. 94, 1105–1110.

Hahn, D.B., Aanstoos, M.E., Wilkins, R.M., 2010. Osteochondral lesions of the talus treated with fresh talar allografts. Foot ankle Int. 31, 277–282. http://dx.doi.org/10.3113/FAI.2010.0277.

Hangody, L., Vásárhelyi, G., Hangody, L.R., Sükösd, Z., Tibay, G., Bartha, L., Bodó, G., 2008. Autologous osteochondral grafting–technique and long-term results. Injury 39 (Suppl. 1), S32–S39. http://dx.doi.org/10.1016/j.injury.2008.01.041.

Hashimoto, S., Nishiyama, T., Hayashi, S., Fujishiro, T., Takebe, K., Kanzaki, N., Kuroda, R., Kurosaka, M., 2009. Role of p53 in human chondrocyte apoptosis in response to shear strain. Arthritis Rheum. 60, 2340–2349. http://dx.doi.org/10.1002/art.24706.

Hollander, A.P., Pidoux, I., Reiner, A., Rorabeck, C., Boume, R., Poole, A.R., 1995. Damage to type II collagen in aging and osteoarthritis starts at the articular surface, originates around chondrocytes, and extends into the cartilage with progressive degeneration. J. Clin. Investig. 96, 2859–2869.

Janis, L., Kaplansky, D.B., DeCarbo, W.T., 2010. Early clinical experience with a fresh talar transplant inlay allograft for the treatment of osteochondral lesions of the talus. J. Am. Podiatr. Med. Assoc.

Juras, V., Bittsansky, M., Majdisova, Z., Szomolanyi, P., Sulzbacher, I., Gäbler, S., Stampfl, J., Schüller, G., Trattnig, S., 2009. In vitro determination of biomechanical properties of human articular cartilage in osteoarthritis using multi-parametric MRI. J. Magn. Reson 197, 40–47. http://dx.doi.org/10.1016/j.jmr.2008.11.019.

Kennedy, J.G., Murawski, C.D., 2011. The treatment of osteochondral lesions of the talus with autologous osteochondral transplantation and bone marrow aspirate concentrate: surgical technique. Cartilage 2, 327–336. http://dx.doi.org/10.1177/1947603511400726.

Kim, Y.S., Park, E.H., Kim, Y.C., Koh, Y.G., Lee, J.W., 2012. Factors associated with the clinical outcomes of the osteochondral autograft transfer system in osteochondral lesions of the talus: second-look arthroscopic evaluation. Am. J. Sport. Med. http://dxdoi.org/10.1177/0363546512461132

Latt, L.D., Glisson, R.R., Montijo, H.E., Usuelli, F.G., Easley, M.E., 2011. Effect of graft height mismatch on contact pressures with osteochondral grafting of the talus. Am. J. Sport. Med. 39, 2662–2669. http://dx.doi.org/10.1177/0363546511422987.

McIlwraith, C.W., Frisbie, D.D., Kawcak, C.E., Fuller, C.J., Hurtig, M., Cruz, A., 2010. The OARSI histopathology initiative - recommendations for histological assessments of osteoarthritis in the horse. Osteoarthr. Cartil. 18 (Suppl. 3). http://dx.doi.org/10.1016/j.joca.2010.05.031.

Meehan, R., Mcfarlin, S., Bugbee, W., Brage, M., 2005. Fresh ankle osteochondral allograft transplantation for tibiotalar joint arthritis. Foot Ankle Int. 26, 793–802.

Mroz, T.E., Joyce, M.J., Steinmetz, M.P., Lieberman, I.H., Wang, J.C., 2008. Musculoskeletal allograft risks and recalls in the United States. J. Am. Acad. Orthop. Surg. 16, 559–565. http://dx.doi.org/10.1215/03616878-25-5-953.

Peng, G., Mcnary, S.M., Athanasiou, K.A., Reddi, A.H., 2015. The distribution of superficial zone protein (SZP)/lubricin/PRG4 and boundary mode frictional properties of the bovine diarthrodial joint. J. Biomech. 48, 3406–3412. http://dx.doi.org/10.1016/j.jbiomech.2015.05.032.

Pritzker, K.P.H., Gay, S., Jimenez, S.A., Ostergaard, K., Pelletier, J.-P., Revell, P.A., Salter, D., van den Berg, W.B., 2006. Osteoarthritis cartilage histopathology: grading and staging. Osteoarthr. Cartil. 14, 13–29. http://dx.doi.org/10.1016/j.joca.2005.07.014.

Quinn, T.M., Häuselmann, H.-J., Shintani, N., Hunziker, E.B., 2013. Cell and matrix morphology in articular cartilage from adult human knee and ankle joints suggests depth-associated adaptations to biomechanical and anatomical roles. Osteoarthr. Cartil. 21, 1904–1912. http://dx.doi.org/10.1016/j.joca.2013.09.011.

Raikin, S.M., 2009. Fresh osteochondral allografts for large-volume cystic osteochondral defects of the talus. J. Bone Jt. Surg. Am. 91, 2818–2826. http://dx.doi.org/10.2106/JBJS.I.00398.

Savage-Elliott, I., Ross, K.A., Smyth, N.A., Murawski, C.D., Kennedy, J.G., 2014. Osteochondral lesions of the talus: a current concepts review and evidence-based treatment paradigm. Foot Ankle Spec. 7, 414–422. http://dx.doi.org/10.1177/1938640014543362.

Saxena, A., Eakin, C., 2007. Articular talar injuries in athletes: results of microfracture and autogenous bone graft. Am. J. Sport. Med. 35, 1680–1687. http://dx.doi.org/10.1177/0363546507303561.

Schinagl, R.M., Gurskis, D., Chen, A.C., Sah, R.L., 1997. Depth-dependent confined compression modulus of full-thickness bovine articular cartilage. J. Orthop. Res. 15, 499–506. http://dx.doi.org/10.1002/jor.1100150404.

Schmidt, T.A., Gastelum, N.S., Nguyen, Q.T., Schumacher, B.L., Sah, R.L., 2007. Boundary lubrication of articular cartilage: Role of synovial fluid constituents. Arthritis Rheum. 56, 882–891. http://dx.doi.org/10.1002/art.22446.

Schumacher, B.L., Su, J.L., Lindley, K.M., Kuettner, K.E., Cole, A.A., 2002. Horizontally oriented clusters of multiple chondrons in the superficial zone of ankle, but not knee articular cartilage. Anat. Rec. 266, 241–248. http://dx.doi.org/10.1002/ar.10063.

Shepherd, D.E., Seedhom, B.B., 1999. Thickness of human articular cartilage in joints of the lower limb. Ann. Rheum. Dis. 58, 27–34. http://dx.doi.org/10.1136/ard.58.1.27.

Silverberg, J.L., Barrett, A.R., Das, M., Petersen, P.B., Bonassar, L.J., 2014. Structure-function relations and rigidity percolation in the shear properties of articular cartilage. Biophys. J. 107, 1721–1730. http://dx.doi.org/10.1016/j.bpj.2014.08.011.

Silverberg, J.L., Dillavou, S., Bonassar, L.J., Cohen, I., 2013. Anatomic variation of depth-dependent mechanical properties in neonatal bovine articular cartilage. J. Orthop. Res. 31, 686–691. http://dx.doi.org/10.1002/jor.22303.

Smith, R.L., Carter, D.R., Schurman, D.J., 2004. Pressure and shear differentially alter human articular chondrocyte metabolism: a review. Clin. Orthop. Relat. Res., S89–S95. http://dx.doi.org/10.1097/01.blo.0000143938.30681.9d.

Takao, M., Uchio, Y., Naito, K., Fukazawa, I., Ochi, M., 2005. Arthroscopic assessment for intra-articular disorders in residual ankle disability after sprain. Am. J. Sport. Med. 33, 686–692. http://dx.doi.org/10.1177/0363546504270566.

Tang, S.Y., Souza, R.B., Ries, M., Hansma, P.K., Alliston, T., Li, X., 2011. Local tissue properties of human osteoarthritic cartilage correlate with magnetic resonance T(1) rho relaxation times. J. Orthop. Res. 29, 1312–1319. http://dx.doi.org/10.1002/jor.21381.

Treppo, S., Koepp, H., Quan, E.C., Cole, A.A., Kuettner, K.E., Grodzinsky, A.J., 2000. Comparison of biomechanical and biochemical properties of cartilage from human knee and ankle pairs. J. Orthop. Res. 18, 739–748. http://dx.doi.org/10.1002/jor.1100180510.

UCLA: Statistical Consulting Group, n.d. Chapter 3: Varying and Random Coefficient Models from Introduction to Multilevel Modeling by Kreft and de Leeuw [WWW Document]. URL ⟨http://www.ats.ucla.edu/stat/stata/examples/mlm_imm/immch3.htm⟩.

Valderrabano, V., Leumann, A., Rasch, H., Egelhof, T., Hintermann, B., Pagenstert, G., 2009. Knee-to-ankle mosaicplasty for the treatment of osteochondral lesions of the ankle joint. Am. J. Sport. Med. 37 (Suppl. 1), 105S–111S. http://dx.doi.org/10.1177/0363546509351481.

Waller, K.A., Zhang, L.X., Elsaid, K.A., Fleming, B.C., Warman, M.L., Jay, G.D., 2013. Role of lubricin and boundary lubrication in the prevention of chondrocyte apoptosis. Proc. Natl. Acad. Sci. USA 110, 5852–5857. http://dx.doi.org/10.1073/pnas.1219289110.

Wong, B.L., Bae, W.C., Chun, J., Gratz, K.R., Lotz, M., Sah, R.L., 2008a. Biomechanics of cartilage articulation: effects of lubrication and degeneration on shear deformation. Arthritis Rheum. 58, 2065–2074. http://dx.doi.org/10.1002/art.23548.

Wong, B.L., Bae, W.C., Gratz, K.R., Sah, R.L., 2008b. Shear deformation kinematics during cartilage articulation: effect of lubrication, degeneration, and stress relaxation. Mol. Cell. Biomech. 5, 197–206.

Wong, B.L., Kim, S.H.C., Antonacci, J.M., McIlwraith, C.W., Sah, R.L., 2010. Cartilage shear dynamics during tibio-femoral articulation: effect of acute joint injury and tribosupplementation on synovial fluid lubrication. Osteoarthr. Cartil. 18, 464–471. http://dx.doi.org/10.1016/j.joca.2009.11.008.

Wong, B.L., Sah, R.L., 2010. Mechanical asymmetry during articulation of tibial and femoral cartilages: Local and overall compressive and shear deformation and properties. J. Biomech. 43, 1689–1695. http://dx.doi.org/10.1016/j.jbiomech.2010.02.035.

Zengerink, M., Struijs, P.A., Tol, J.L., van Dijk, C.N., 2010. Treatment of osteochondral lesions of the talus: a systematic review. Knee Surg. Sport. Traumatol. Arthrosc. 18, 238–246. http://dx.doi.org/10.1007/s00167-009-0942-6.